# Serum- and Glucocorticoid-Inducible Kinase 1 (SGK1) Increases Neurite Formation through Microtubule Depolymerization by SGK1 and by SGK1 Phosphorylation of tau[▽]

Ying C. Yang,[1] Cheng H. Lin,[2] and Eminy H. Y. Lee[1]*

*Division of Neuroscience, Institute of Biomedical Sciences, Academia Sinica,[1] and Graduate Institute of
Life Sciences, National Defense Medical Center,[2] Taipei, Taiwan, Republic of China*

**Serum- and glucocorticoid-inducible kinase 1 (SGK1) is a member of the Ser/Thr protein kinase family that regulates a variety of cell functions. Recently, SGK1 was shown to increase dendritic growth but the mechanism underlying the increase is unknown. Here we demonstrated that SGK1 increased the neurite formation of cultured hippocampal neurons through microtubule (MT) depolymerization via two distinct mechanisms. First, SGK1 directly depolymerized MTs. In vitro MT depolymerization experiments revealed that SGK1, especially N-truncated SGK1, directly disassembled self-polymerized MTs and taxol-stabilized MTs in a dose-dependent and ATP-independent manner. The transfection of *sgk1* to HeLa cells also inhibited MT assembly in vivo. Second, SGK1 indirectly depolymerized MTs through the phosphorylation of tau at Ser214. An in vitro kinase assay revealed that active SGK1 phosphorylated tau Ser214 specifically. In vivo transfection of *sgk1* also phosphorylated tau Ser214 in HEK293T cells and hippocampal neurons. Further, *sgk1* transfection significantly increased the number of primary neurites and shortened the length of the total process in cultured hippocampal neurons. These effects were antagonized by the cotransfection of the *tau*S214A mutant plasmid. Dexamethasone, a synthetic glucocorticoid, mimics the effect of *sgk1* overexpression. Together, these results suggest that SGK1 enhances neurite formation through MT depolymerization by a direct action of SGK1 and by the SGK1 phosphorylation of tau.**

Neurons are terminally postmitotic cells that use their microtubules (MTs) for the formation of neuronal processes other than the formation of a mitotic spindle. Structural plasticity mediated by MT dynamics is responsible for important neuronal events, such as process elongation, branching, guidance, retraction, pruning, learning, and memory formation (12, 17, 47, 50). MT dynamics, which are composed of catastrophes and rescues, are dependent on the relative speed between polymerization and depolymerization at the MT plus and minus ends.

Two groups of proteins, MT stabilizers and destabilizers, are the best-characterized cellular factors that regulate MT dynamics in cells (22). MT stabilizers, such as microtubule-associated protein (MAP), stabilize MTs mainly by binding to the sides of MTs to suppress catastrophes and increase rescues (8, 9). MAP is required for neurite formation (18); however, an elevated level of MAP, which leads to abnormal MT stability, is related to the pathogenesis of fragile X mental retardation syndrome (38). Tau, a neuronal MAP, is involved in the regulation of neurite formation (7); however, the overexpression of tau in *Drosophila melanogaster* impairs associated learning and memory (45) and leads to neurodegeneration (14). The kinetics of MTs suggest that MT dynamic instability, rather than net polymerization, is important for determining the influence of MT on brain function. In fact, an MT turns over

more rapidly in vivo than an MT assembled from pure tubulin in vitro (27). Therefore, the discovery of MT destabilizers, such as katanin (44), stathmin (4), SCG10 (49), kin I kinesin (13), and spastin (51, 55), is very important. MT destabilizers have also been shown to affect neuronal development and neuronal function. For example, an injection of katanin antibody (Ab) was found to inhibit axon outgrowth (1), whereas the overexpression of its active subunit results in a loss of MT mass and shortening of the total process length (62). Stathmin knockout mice develop axonopathy in the central nervous system and the peripheral nervous system (36). Further, the loss of spastin in *Drosophila* causes an aberrantly stabilized MT and defects in synaptic growth and neurotransmissions (55). Thus, both MT stabilizers and destabilizers are required for neurite outgrowth and normal brain function.

Serum- and glucocorticoid-inducible kinase 1 (SGK1), which belongs to the AGC subfamily of the Ser/Thr protein kinases, contains a catalytic (cat.) domain that is approximately 45 to 55% homologous to that of AKT but lacks the pleckstrin homology (PH) domain present in AKT (16). The *sgk1* gene is highly conserved from yeast (*Saccharomyces cerevisiae*) to human, and the SGK1 protein is regulated in a tissue- and stage-specific pattern during embryogenesis and postnatal development. At late stages (E13.5 through E16.5) of mouse embryogenesis, SGK1 expression becomes highly concentrated in the brain (33). SGK1 was originally identified by its transcriptional regulation by serum and glucocorticoid (57) and its activation by insulin-induced phosphatidylinositol 3-kinase (PI3K) activation (48). Less is known about the role of SGK1 in the central nervous system. More recently, SGK1 was found to play an important role in spatial memory formation (32, 56),

* Corresponding author. Mailing address: Division of Neuroscience, Institute of Biomedical Sciences, Academia Sinica, Taipei 115, Taiwan. Phone: 886-2-2789-9125. Fax: 886-2-2782-9224. E-mail: eminy@gate.sinica.edu.tw.

long-term potentiation (39), and neuronal plasticity induced by environmental enrichment training (34). It is known that memory formation is a process accompanied by the reorganization of preexisting structures and the formation of new connections (47, 58). More related to the present study, the transfection of constitutively active *sgk1* was shown to cause dendritic growth and dendritic branching in spinal cord neurons (11). However, the molecular mechanism underlying SGK1-induced dendritic growth is not known. In tumor cells, SGK1 is predominantly nuclear associated in the S and $G_2$/M phases regulating cell cycle progression (6). Clinically, pretreatment with dexamethasone, a synthetic glucocorticoid, inhibits antimitosis induced by the chemotherapeutic drug paclitaxel (Taxol) and this effect is mediated by SGK1 through unknown mechanisms (59). These results suggest that SGK1 may regulate the cell cycle through the modulation of MT dynamics in tumor cells. Because MT dynamics play a major role in most process formations (12, 50), we proposed a role of SGK1 in the regulation of MT plasticity. In the present study, we examined whether SGK1 increases the neurite formation of cultured hippocampal neurons through the modulation of MT depolymerization. Our results revealed that SGK1 depolymerizes MTs through two distinct mechanisms both in vitro and in vivo. First, SGK1 directly depolymerizes MT independently of its kinase activity. Second, SGK1 depolymerizes MT through the phosphorylation of tau specifically at Ser214.

## MATERIALS AND METHODS

**Plasmid construction.** For the construction of enhanced green fluorescent protein (EGFP)-tagged SGK1, rat full-length (FL) *sgk1* was amplified from the pcDNA3-*sgk1* plasmid (56) and human *sgk1* was cloned from cDNA of HEK293T cells. The *sgk1* insert was subcloned into BglII/EcoRI sites of the pEGFP-N3 vector (Clontech, Mountain View, CA). To generate the kinase-dead *sgk1* K127M construct of *sgk1*, pcDNA3-*sgk1* was first denatured to single-strand DNA by the alkaline denaturation method (0.2 M NaOH and 0.2 mM EDTA). Lys127 was mutated to Met (underlined) by PCR with primers 5′-GAA GCA TTC TAT GCC GTC ATG GTT TTG CAG AAG AAA GCC ATC TTG-3′ and 5′-CAA GAT GGC TTT CTT CTG CAA AAC CAT GAC GGC ATA GAA TGC TTC-3′. The PCR parameters used were 95°C for 30 s, 55°C for 1 min, and 68°C for 4.5 min for 16 cycles, followed by DpnI digestion and then transformation to *Escherichia coli*. The sequence of the mutant construct was confirmed by DNA sequencing. For the construction of glutathione *S*-transferase (GST)-tagged SGK1, the amplified rat full-length *sgk1* was inserted into the EcoRI/XhoI sites of the pGEX-4T1 expression vector (Amersham Pharmacia Biotech, Piscataway, NJ). The various fragments of SGK were designed as previously described (41). Human full-length *tau* (441 amino acids [aa]) containing a XhoI/EcoRI site was amplified from pET-28a-*tau* (a gift from P. J. Lu, Kaohsiung, VG Hospital, Taiwan) and was subcloned into the pRSET-A (Invitrogen, Carlsbad, CA) or pDsRed2-N1 vector (Clontech). The PCR was performed at 95°C for 30 s, 55°C for 1 min, and 68°C for 1.5 min for 30 cycles in the presence of 5% dimethyl sulfoxide and 1 M betaine (Sigma-Aldrich, St. Louis, MO). To mutate tau Ser214 to Ala, pRSET-*tau* was denatured and mutated as described above. The mutation was generated by PCR with primers 5′-GGC AGC CGC TCC CGC ACC CCG GCC CTT CCA ACC CCA CCC ACC CG-3′ and 5′-CGG GTG GGT GGG GTT GGA AGG GCC GGG GTG CGG GAG CGG CTG CC-3′. The PCR parameters were 95°C for 30 s, 55°C for 1 min, and 68°C for 4.5 min for 16 cycles in the presence of 5% dimethyl sulfoxide and 1 M betaine, followed by DpnI digestion and transformation to *E. coli*. After sequence confirmation, the *tau*S214A insert was subcloned into the XhoI/EcoRI sites of pDsRed2-N1. To construct *sgk1* short hairpin RNA (shRNA), the pSUPER plasmid (a gift from C.-Y. F. Huang, NHRI, Taiwan) with an H1 promoter was used to express the shRNA targeted against the rat *sgk1* gene. To visualize cells with successful transfection, the EGFP sequence was inserted into pSUPER under the control of a cytomegalovirus promoter. The effective target sequence was constructed according to a previously reported short interfering RNA sequence against *sgk1* (59). The corresponding oligonucleotide sequences (*sgk1* forward

oligonucleotides consisted of 5′-gatccccGTCCCTCTCAACAAATCAAttcaagag aTTGATTTGTTGAGAGGGACttttttggaaa-3′, and *sgk1* reverse oligonucleotides consisted of 5′-agcttttccaaaaaGTCCCTCTCAACAAATCAAtctcttgaaTTG ATTTGTTGAGAGGGACggg-3′) were synthesized, annealed, digested with BglII and HindIII, and ligated into the pSUPER vector as described previously (5). Restriction and DNA-modifying enzymes were purchased from New England Biolabs (Beverley, MA), Stratagene (La Jolla, CA), or Promega (Madison, WI).

**Cells.** To culture embryonic hippocampal primary neurons, pregnant Sprague-Dawley rats bred in the Institute of Biomedical Sciences, Academia Sinica, in Taiwan, were housed one per cage in a temperature-regulated room (23 ± 2°C) and maintained on a 12-h light-dark cycle (lights on at 6:30 a.m.) with food and water continuously available. All procedures were adopted according to the Guidelines of Animal Use and Care from the National Institutes of Health. The hippocampal tissue from embryos of Sprague-Dawley rats (E19) was dissociated with 100 U/ml papain and plated onto poly-L-lysine-coated coverslips at a density of $1 \times 10^4$ cells/cm² with minimal essential medium containing 5% calf serum, 5% horse serum, and 50 ng/ml insulin-transferrin-selenite (Sigma-Aldrich). Three hours after plating, the medium was replaced with 2% B27-neurobasal medium (Invitrogen) containing 0.5 mM glutamine and 12.5 μM glutamate. HEK293T and HeLa cells were maintained in Dulbecco's modified Eagle's medium supplemented with 10% fetal calf serum. Cultures were maintained in a humidified 5% $CO_2$-95% air atmosphere at 37°C.

**Transfection.** For the transfection of hippocampal neurons at day in vitro (DIV) 0, dissociated hippocampal neurons were resuspended in Nucleofector solution (Amaxa Biosystems, Cologne, Germany) and plasmid DNA was transfected with an electroporator nucleofection device (Amaxa Biosystems) as instructed. For HEK293T and HeLa cells, Lipofectamine 2000 reagent (Invitrogen) was used for the transfection of plasmids to cultured hippocampal neurons at DIV 2 and DIV 9.

**Immunofluorescence and neurite estimation.** Cultured hippocampal neurons were fixed with 4% paraformaldehyde-4% sucrose for 15 min and permeabilized with 0.1% Triton X-100 for 20 min at room temperature (RT). The primary Abs, rabbit anti-SGK1 (UBI, Lake Placid, NY) and anti-tau [pSer²¹⁴] (Biosource, Camarillo, CA) Abs, were added for overnight at 4°C. Mouse anti-β III tubulin (Promega) or anti-tau (Biosource) Abs were added for 1 h at RT. After wash, Alexa Fluor 488 goat anti-rabbit Ab (Molecular Probes, Leiden, Netherlands) and Cy3 and Cy5 donkey anti-mouse Abs (Jackson Laboratory, West Grove, PA) were incubated with cells for 1 h at RT. Coverslips were mounted, and images were obtained by using a confocal microscope (MRC 1000; Bio-Rad, Hercules, CA). For neurite estimation, plasmid-transfected hippocampal neurons were fixed as described above. Neurons were stained with mouse anti-β III tubulin Ab (Promega) for process measurement, and images were analyzed by using Confocal Assistant software (Bio-Rad) and Metamorph software (Molecular Devices, Sunnyvale, CA). Primary neurite is a neurite that arises from the cell body. The number of neurites was determined by counting the number of primary neurites that were longer than 5 μm. HeLa cells were fixed with 3.7% paraformaldehyde for 10 min at RT and permeabilized with 0.1% Triton X-100 for 5 min (25). Monoclonal anti-β III tubulin Ab (Sigma-Aldrich) and Cy3 donkey anti-mouse Abs were used for immunostaining as described above.

**Immunoprecipitation.** Hippocampal neurons were lysed with phosphate-buffered saline buffer containing 1% NP-40, 0.5% Na-deoxycholate, 0.1% sodium dodecyl sulfate (SDS), 1 mM $Na_3VO_4$, 10 mM NaF, 1 mM phenylmethylsulfonyl fluoride (PMSF), 20 μg/ml pepstatin A, 20 μg/ml leupeptin, and 20 μg/ml aprotinin and were scraped from the dish, followed by centrifugation at 14,000 rpm for 5 min. The supernatant (S1) was kept, and the pellet (P1) was added with 10 to 20 μl lysis buffer. After pipetting and sonication, the P1 lysate was separated into S2 and P2 fractions after another centrifugation. The S1 and S2 fractions were then pooled as the total protein. For immunoprecipitation, 1,500 μg of cell lysate was precleared with nonimmunized immunoglobulin G and protein G-Sepharose (Amersham Pharmacia Biotech) twice. To avoid heavy chain interference during SDS-polyacrylamide gel electrophoresis (PAGE), anti-tau Ab and anti-SGK1 Ab were cross-linked to protein G-Sepharose by disuccinimidyl suberate (Pierce, Rockford, IL). Precleared lysate and anti-tau-protein G–Sepharose or anti-SGK1-protein G–Sepharose Ab was incubated for 1.5 h at RT, and the immunoprecipitate was subjected to an immunoblotting assay.

**Immunoblotting.** Neurons transfected with pSUPER-*sgk1* shRNA were subjected to either the fluorescence-activated cell sorter FACSVantage SE (BD Pharmingen, San Diego, CA) for immunoblotting or an immunofluorescence assay 48 h later. Immunoblotting was performed as described previously (60). In brief, neurons were lysed and scraped in buffer containing 50 mM Tris-HCl, pH 8.0, 150 mM NaCl, 2 mM EDTA, 1 mM $Na_3VO_4$, 10 mM NaF, and 1 mM PMSF plus 1% NP-40 and 20 μg/ml pepstatin A, 20 μg/ml leupeptin, and 20 μg/ml

aprotinin. The lysate was centrifuged at $14,000 \times g$ for 10 min at 4°C to get the crude cytosolic fraction. HEK293T cells were lysed in HEPES buffer containing 150 mM NaCl, 5 mM EDTA, 10 μg/ml aprotinin, 5 μg/ml leupeptin, 10% glycerol, and 1% Triton X-100. Equal amounts of extract were subjected to SDS-PAGE and transferred to a polyvinylidene difluoride membrane (Millipore, Bedford, MA). The primary Abs used were rabbit polyclonal anti-SGK1 Ab (UBI), a polyclonal anti-phospho-tau Ab kit containing pThr181, pSer202, pThr205, pThr212, pSer214, pThr231, pSer262, pSer396, pSer404, pSer409, and pSer422 (Biosource), mouse monoclonal anti-β actin Ab (UBI), anti-tau Ab (Biosource), anti-β III tubulin Ab (Promega), anti-DsRed Ab (BD Pharmingen, San Diego, CA), and rat monoclonal anti-hemagglutinin (HA) Ab (Roche Diagnostics, Mannheim, Germany). After incubation with the specific primary Ab, horseradish peroxidase-conjugated secondary Ab was added and visualized via chemiluminescence (Amersham Biosciences). For reprobing, the blot was stripped in 0.2 M glycine, pH 2.5, and 0.05% Tween 20 at 80°C for 30 min and then rinsed twice with 90 mM boric acid, pH 7.4, 0.9% NaCl, and 0.05% Tween 20.

**Drug treatment.** Dexamethasone (1 μM; Sigma-Aldrich), a synthetic glucocorticoid, was applied to cultured hippocampal neurons at DIV 5. Twenty-four hours later, cultured neurons were fixed and immunostained with mouse anti-β III tubulin Ab for neurite observation and measurement as described above. In different batches of cultures, cells were collected and processed for Western blot analyses of SGK1, SGK1-pSer422, tau, tau-pSer214 and β-actin.

**Protein purification.** The human full-length pET-28a-*tau* was transformed to *E. coli* BL21 cells for expression. After an induction with IPTG (isopropyl-β-D-thiogalactopyranoside) (1 mM) for 1.5 h at 27°C, cells were collected and sonicated in binding buffer (20 mM Tris-HCl, pH 7.9, 0.5 M NaCl, 5 mM imidazole, 2 mg/ml lysozyme, 1 mM PMSF, 2 μg/ml aprotinin, and 2 μg/ml leupeptin). After centrifugation at 13,000 rpm for 20 min, the supernatant was filtered with a 0.45-μm syringe filter and applied to a ProBond Ni-resin column (Bio-Rad). The His-tau protein was eluted with 0.5 M imidazole, dialyzed with BC-100 buffer (20 mM Tris-HCl, pH 8, 0.2 mM EDTA, 100 mM KCl, 20% glycerol, 0.5 mM dithiothreitol, and 0.2 mM PMSF), and concentrated by Centricon (Millipore, Bedford, MA). The rat pGEX-*sgk1* fragment constructs were transformed and induced as pET-28a-*tau*, followed by sonication in buffer containing 50 mM NaH$_2$PO$_4$, pH 8, 0.3 M NaCl, 20% glycerol, 2 mg/ml lysozyme, 1 mM PMSF, 2 μg/ml aprotinin, and 2 μg/ml leupeptin. After centrifugation, the GST-SGK1 protein was incubated with glutathione-Sepharose beads (Amersham Pharmacia Biotech), eluted with 10 mM of reduced glutathione, and then dialyzed and concentrated as pET-28a-*tau*.

**Kinase assay.** For an in vitro kinase assay, purified His-tau or His-TauS214A (1 μg) was incubated with active SGK1 (100 ng, 40 ng/μl; UBI) in a total volume of 40 μl kinase buffer (25 mM Tris-HCl, pH 7.5, 5 mM β-glycerophosphate, 2 mM dithiothreitol, 0.1 mM Na$_3$VO$_4$, 10 mM MgCl$_2$, and 100 μM ATP and 8 μCi [γ-$^{32}$P]ATP) for 10 min at 30°C. The reaction was stopped by adding the protein sample buffer and heating for 10 min at 95°C. Twenty microliters of the sample was loaded to 8% SDS-PAGE gels for autoradiography to determine the level of tau phosphorylation. Tau was immunoprecipitated as described above, and the immunoprecipitate was separated into aliquots for subsequent kinase assays.

**MT polymerization assay.** Pure bovine brain tubulin (35 μM or 70 μM; Cytoskeleton, Denver, CO) was incubated with equal molars (0.2 μM) of N-terminally truncated SGK1 (ΔN-SGK1), SGK1 K127M, AKT (UBI), and myelin basic protein (MBP) (UBI) to a final volume of 130 μl in GPEM buffer {80 mM PIPES [piperazine-*n,n'*-bis(2-ethanesulfonic acid)] at pH 6.8, 1 mM EGTA, 1 mM MgCl$_2$, 1 mM GTP, and 10% glycerol}. Absorbance at 340 nm was read by a U2000 spectrophotometer (Hitachi, Tokyo, Japan) for 50 min at 37°C. For active SGK1 (UBI) phosphorylation of tau (3.8 μM) or TauS214A (3.8 μM), a kinase reaction was carried out for 10 min at 30°C and the mixture was added to the cuvette containing tubulin (35 μM) for spectrophotometric analysis. After 50 min of recording, the mixture was fixed by adding 400 μl of 1% glutaraldehyde in GPEM buffer, sedimented through a 25% glycerol cushion (in RG1 buffer, which contained 80 mM PIPES, pH 6.8, 1 mM EGTA, 1 mM MgCl$_2$, and 1 mM GTP), postfixed with methanol-acetone (1:1) for 10 min at −20°C, and examined under a confocal microscope by using anti-β III tubulin Ab (Promega).

**MT reassembly assay.** HeLa cells were transfected with pEGFP-human *sgk1* fragment constructs by Lipofectamine 2000 reagent. Twenty-four hours later, transfected cells were incubated for 1 h at 4°C and immediately replaced by warm medium for 10 min at 37°C (25). Cells were then fixed with 3.7% paraformaldehyde for 10 min at RT and permeabilized with 0.1% Triton X-100 for 5 min. Monoclonal anti-β III tubulin (Sigma-Aldrich) and Cy3 donkey anti-mouse Abs were used for immunostaining as described above.

**MT sedimentation assay.** Pure bovine brain tubulin (16 μM; Cytoskeleton) was prepolymerized with 25 μM Taxol (Sigma-Aldrich) for 10 min at 37°C in RG1 buffer containing 4 mM MgCl$_2$ and 1 mM GTP. Equal molars (0.2 μM) of ΔN-SGK1, AKT, and MBP were added to prepolymerized MT and incubated for another 10 min at 37°C. The reaction mixture was centrifuged through a 50-μl glycerol cushion (50% glycerol, 25 μM Taxol, and 1 mM GTP in RG1 buffer) at $100,000 \times g$ for 30 min at 37°C in a Beckman TL-100 ultracentrifuge. The fractions containing the supernatant and the pellet were subjected to 10% SDS-PAGE, followed by immunoblotting with anti-SGK1 (UBI) and anti-β III tubulin (Promega) Abs.

## RESULTS

**SGK1 increases neurite formation of hippocampal neurons.** To investigate whether SGK1 affects neurite outgrowth, pEGFP-*sgk1* was first transfected to cultured hippocampal neurons at stages DIV 2 and DIV 9 and neuronal morphology was examined 24 h later. Results shown in Fig. 1A revealed that *sgk1* transfection induced a complex elaboration of dendrites and a small-caliber axon at these developmental stages. This observation is similar to that of a recent report showing that constitutively active *sgk1* increases dendritic growth and dendritic branching of spinal cord neurons (11). To better assess the effect of SGK1 on neurite outgrowth, pEGFP-*sgk1* was transfected to cultured hippocampal neurons at DIV 0, an earlier developmental stage that manifests process outgrowth more clearly. The results revealed that vector-transfected neurons showed longer neurites, and these neurites elongated into asymmetric polarity, in which one would develop into an axon (Fig. 1B). Meanwhile, the transfection of *sgk1* at this stage significantly increased the number of primary neurites approximately twofold ($t_{1,\,63} = 4.63$, where $t$ indicates Student's $t$ test; $P < 0.01$) (Fig. 1B and C). These neurites appeared in a tapered, symmetric array that lost elongated neurite extension (Fig. 1B). On the other hand, *sgk1* transfection decreased the length of the total neurite process by approximately 60% ($t_{1,\,63} = 6.6$; $P < 0.01$) (Fig. 1B and D). If the overexpression of SGK1 enhances neurite formation, then a decrease in the SGK1 level should inhibit this effect. We tested this hypothesis by transfecting pSUPER-*sgk1* shRNA to cultured hippocampal neurons to knock down SGK1 expression. In order to visualize the transfected cells, a sequence encoding EGFP was inserted into pSUPER under the control of a cytomegalovirus promoter. The results revealed that the neurites of *sgk1* shRNA-transfected neurons appeared to twist around in the vicinity of the cell body instead of extending away from the cell body (Fig. 1E). Further analyses indicated that *sgk1* shRNA transfection markedly decreased the number of primary neurites ($t_{1,\,27} = 2.18$; $P < 0.05$) (Fig. 1F) and increased the length of the total process ($t_{1,\,27} = 2.05$; $P < 0.05$) (Fig. 1G) in cultured hippocampal neurons.

**SGK1 is concentrated at regions devoid of stabilized MT and is associated with tau.** It is known that neuronal morphogenesis is driven by cytoskeletal changes in which MT plays a leading role (3). In studying the relationship between SGK1 and MT, we found that SGK1 is not only associated with stabilized MT but also concentrated at regions devoid of stabilized MT (Fig. 1H, upper and lower panels). This distribution pattern suggests that SGK1 may affect MT organization. In addition, because a substrate motif for SGK1 is found in tau and tau is well known for its role in neuronal MT stabilization and axon formation (54), we also examined the role of tau in
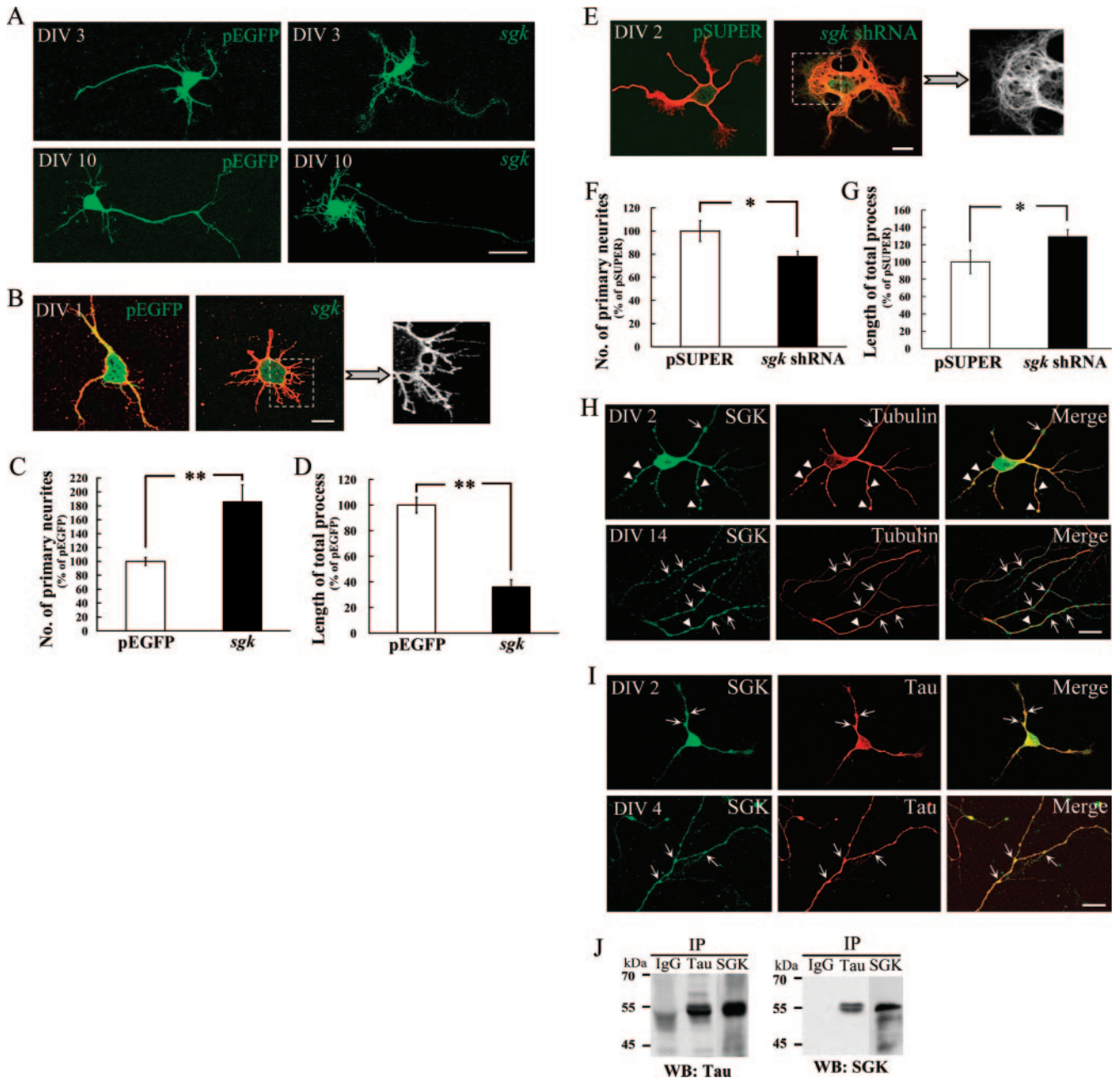
FIG. 1. SGK1 increases neurite formation of hippocampal neurons. (A) Cultured hippocampal neurons were transfected with pEGFP-*sgk1* at DIV 2 and DIV 9 and were fixed at DIV 3 and DIV 10, respectively. The EGFP-SGK1 protein expression was directly observed with a confocal fluorescence microscope. Scale bar, 20 μm. (B) Hippocampal neurons were transfected with pEGFP-*sgk1* at DIV 0 and fixed at DIV 1. Neuronal processes were visualized by immunostaining with anti-β III tubulin Ab (red). The EGFP-SGK1 protein expression was readily observed with a confocal fluorescence microscope. Scale bar, 10 μm. (C and D) The transfection of pEGFP-*sgk1* at DIV 0 significantly increased the number of primary neurites but decreased the length of the total process. $n = 44$ and 21 for pEGFP and pEGFP-*sgk1* groups, respectively. Error bars indicate standard errors of the means. ∗∗, $P$ was <0.01 compared with that of the control vector group. (E) Hippocampal neurons were transfected with pSUPER or pSUPER-*sgk1* shRNA at DIV 0 and were fixed at DIV 2. Neuronal processes were visualized by immunostaining with anti-β III tubulin Ab (red). Scale bar, 10 μm. (F and G) The transfection of *sgk1* shRNA decreased the number of primary neurites but increased the length of the total process. $n = 10$ and 19 for pSUPER and pSUPER-*sgk1* shRNA groups, respectively. Error bars indicate standard errors of the mean. ∗, $P$ was <0.05 compared with that of the control vector group. (H) Cultured hippocampal neurons were coimmunostained with SGK1 and tubulin Abs for confocal microscopic imaging. Endogenous SGK1 (green) is not only associated with MT (red) (arrowheads and yellow color) but also concentrated at regions devoid of stabilized MT (arrows and green color). The upper panels show DIV 2, and the lower panels show DIV 14. Scale bar, 20 μm. (I) SGK1 (green) is highly associated with tau (red) (arrows and yellow color). The upper panels show DIV 2, and the lower panels show DIV 4. Scale bar, 20 μm. (J) Endogenous tau and SGK1 were coimmunoprecipitated with each other. Anti-tau-protein G–Sepharose cross-linked Ab and anti-SGK1-protein G–Sepharose cross-linked Ab were incubated with 1,500 μg rat hippocampal lysate and subjected to 8% SDS-PAGE. PVDF membrane was probed with Abs specific for SGK1 and tau. Data are expressed as means ± standard errors of the means. Statistics were determined by Student's $t$ test. IP, immunoprecipitate; WB, Western blot. IgG, immunoglobulin G.

SGK1-regulated neurite formation. Immunostaining results revealed that SGK1 is highly associated with tau in neuronal processes at both DIV 2 (Fig. 1I, upper panel) and DIV 4 (Fig. 1I, lower panel). The coimmunoprecipitation experiment confirmed the association between SGK1 and tau in hippocampus neurons (Fig. 1J). This result suggests that SGK1 may interact with tau during process outgrowth.

**Identification of the SGK1 fragments that depolymerize MTs.** In this experiment, we examined whether SGK1 may directly act on MT by carrying out an in vitro MT polymerization assay. A higher concentration of purified brain tubulin (70 μM) was used because MT self-polymerization takes place at this concentration at 37°C (Fig. 2B). To determine the effective fragments of SGK1 that depolymerize MT, we examined the effect of a series of GST-fusion *sgk1* constructs, including GST-tagged full-length SGK1, ΔN-SGK1 (aa 1 to 59 were truncated), ΔC-SGK1 (aa 356 to 431 were truncated), catalytic domain-only SGK1 (aa 60 to 355) and C-terminal-only SGK1 (aa 356 to 431), according to the design of a previous study (41). Purified GST-SGK1 fragment proteins were subjected to SDS-PAGE, followed by Coomassie blue staining (Fig. 2A, lanes 1 through 6). After the incubation of various SGK1 fragments with self-polymerized MT, the reaction mixture was ultracentrifuged to coverslips and immunostained with anti-β III tubulin Ab. The results revealed that ΔN-SGK1 (0.4 μM) depolymerized MT into dotted precipitant most effectively (Fig. 2B). Equal molars (0.4 μM) of FL and cat. domain SGk1 and ΔC-SGK1 also depolymerized MT into short fragments, and partial MT depolymerization was observed with C-terminal-only SGK1 (Fig. 2B). These results suggest that SGK1 directly depolymerizes MT in vitro and ΔN-SGK1 is the most effective fragment that depolymerizes MT.

SGK1 directly disassembles self-polymerized MT and Taxol-induced prepolymerized MT independently of its kinase activity. Because SGK1 is a Ser/Thr protein kinase, in the present experiment, we examined whether SGK1 kinase activity is required for the MT depolymerization effect of SGK1. Spectrophotometric recording was adopted because MT formation in tubulin polymerization buffer can be measured by using continuous spectrophotometric recording with absorbance at 340 nm (20). Equal molars (0.2 μM) of ΔN-SGK1, SGK1 K127M, AKT, and MBP were incubated with self-polymerized MT (70 μM) and subjected to spectrophotometric recording for 50 min. At the end of recording, the reaction mixture was ultracentrifuged on coverslips and immunostained with anti-β III tubulin Ab. Results from both experiments revealed that ΔN-SGK1 disassembled MT into fragments in both the presence and the absence of ATP (Fig. 3A). Although ATP was not present in the above MT polymerization assay, the possibility that SGK1 may use GTP as the phosphate donor cannot be ruled out. To further examine the requirement of SGK1 kinase activity, the effect of a kinase-deficient mutant of SGK1, in which Lys127 was replaced with Met (47), was studied. The results revealed that equal molars (0.2 μM) of SGK1 K127M also effectively disassembled MTs into fragments (Fig. 3A). To examine the specificity of SGK1 on MT depolymerization, we also studied the effect of AKT, an SGK homologue, on MT depolymerization. The results revealed that AKT did not disassemble self-polymerized MT as did SGK1 (Fig. 3A). In addition, we adopted an irrelevant protein as a positive control to
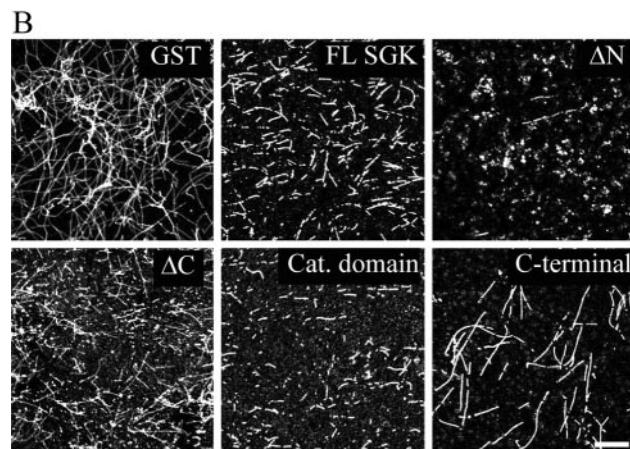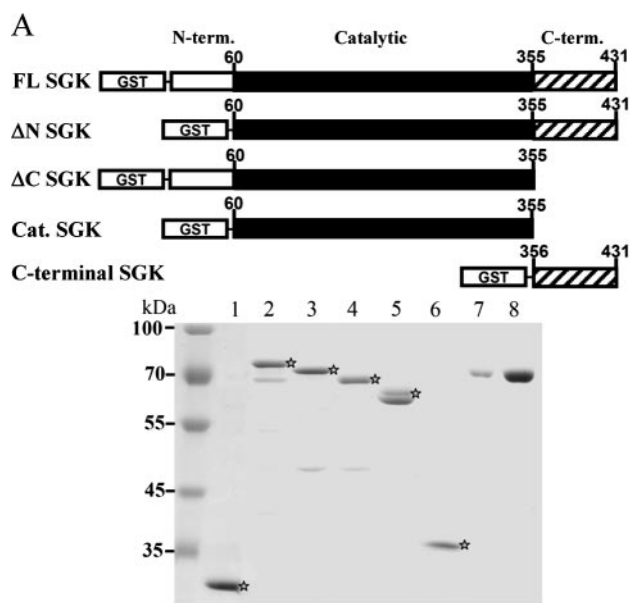


FIG. 2. Identification of the SGK1 fragments that depolymerize MT. (A) Schematic diagram showing SGK1 fragments. cDNA constructs containing fragments of SGK1 were subcloned into the pGEX4T-1 vector and expressed as GST-SGK1-truncated proteins in *E. coli*, followed by a Sepharose affinity purification method. Equal amounts of GST-SGK1 fragments (0.4 μM) and purified bovine serum albumin (BSA) proteins were subjected to 8% SDS-PAGE, followed by Coomassie brilliant blue staining. Lane 1, GST; lane 2, GST-FL-SGK1; lane 3, GST-ΔN-SGK1 (aa 1 to 59 were truncated); lane 4, GST-ΔC-SGK1 (aa 356 to 431 were truncated); lane 5, GST-cat. domain-SGK1 (aa 60 to 355); lane 6, GST-C-terminal SGK1 (aa 356 to 431); lane 7, BSA (1 μg); lane 8, BSA (3 μg). term., terminal. ☆, various SGK fusion proteins. (B) ΔN-SGK1 is the most effective fragment for depolymerizing MT. A high concentration of tubulin was incubated with equal molars of GST- and GST-SGK1-truncated proteins in tubulin polymerization buffer for 50 min at 37°C. The reaction mixture was then ultracentrifuged onto coverslips and immunostained with anti-β III tubulin Ab, followed by confocal microscopic observation. Scale bar, 40 μm.

further examine the specificity of SGK1 on MT depolymerization. Since MBP was known to stabilize MT and induce MT bundle formation (23), it was used as a control agent in the present experiment. The results revealed that equal molars (0.2 μM) of MBP effectively increased MT bundle formation
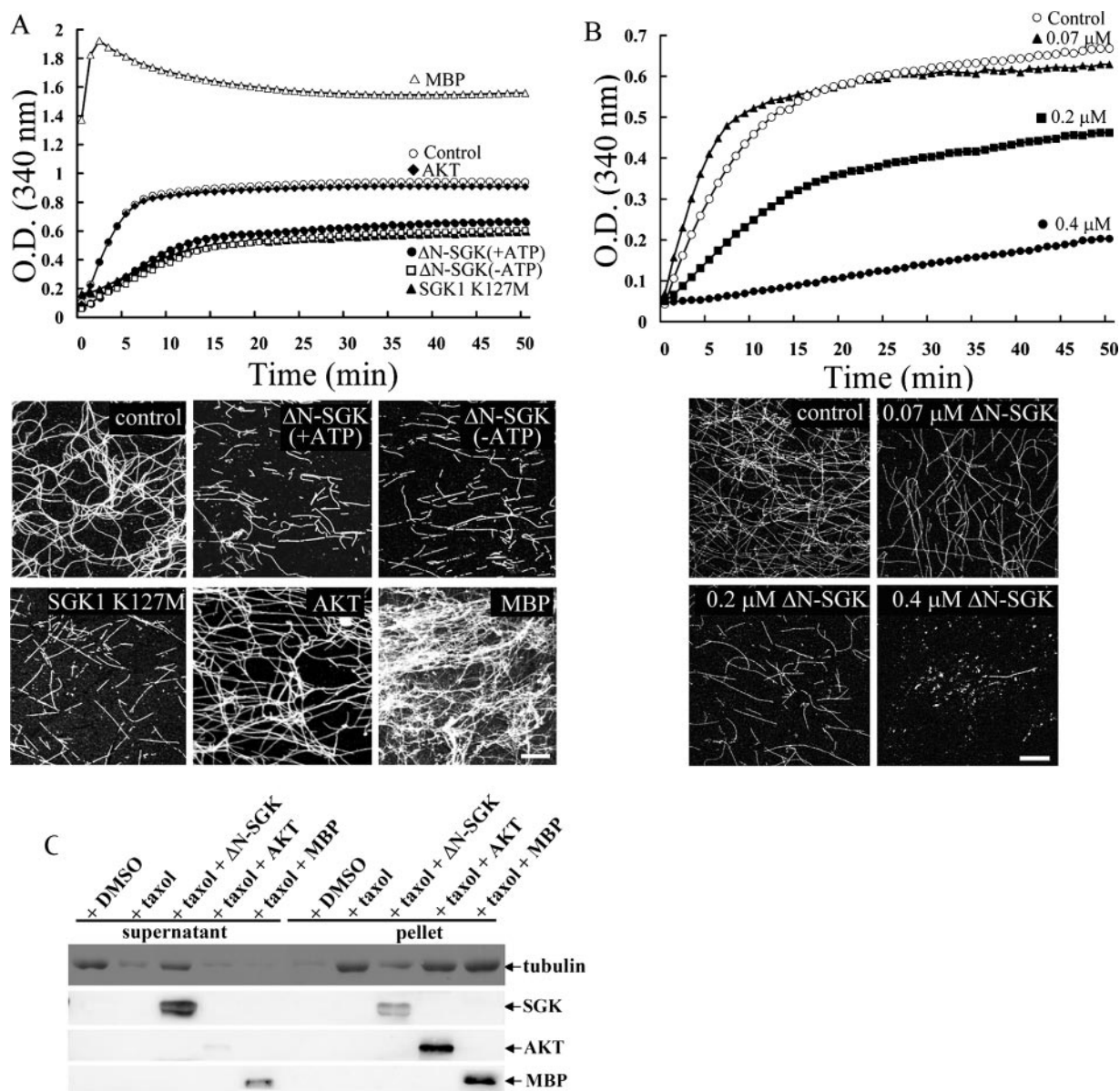
FIG. 3. SGK1 directly and dose dependently disassembles self-polymerized MT and Taxol-stabilized MT independently of its kinase activity. (A) A high concentration of tubulin-induced self-polymerization (○) was suppressed by ΔN-SGK1 in either the presence of ATP (+ATP) or the absence of ATP (−ATP). The kinase-dead SGK1, SGK1 K127M, also caused MT depolymerization in the absence of ATP. Purified AKT had no effect, whereas MBP enhanced MT polymerization in the absence of ATP (upper panel). After 50 min of spectrophotometric recording, the reaction mixture was centrifuged onto coverslips and immunostained with anti-β III tubulin Ab (lower panel). ΔN-SGK1 and SGK1 K127M both shortened the length and decreased the density of MT. AKT had no significant effect on self-polymerized MT, whereas MBP promoted MT bundle formation. Scale bar, 40 μm. O.D., optical density. (B) A high concentration of tubulin-induced self-polymerization is dose dependently inhibited by 0.07 μM, 0.2 μM, and 0.4 μM of ΔN-SGK1 in the absence of ATP (upper panel). After 50 min of spectrophotometric recording, the reaction mixture was immunostained with anti-β III tubulin Ab (lower panel). Scale bar, 40 μm. O.D., optical density. (C) A low concentration of tubulin was prepolymerized by the addition of Taxol. ΔN-SGK1, AKT, or MBP was then added to Taxol-stabilized MT in the absence of ATP. The reaction mixture was ultracentrifuged, and equal volumes of the supernatant and pellet fractions were subjected to 8% SDS-PAGE. Immunoblotting was carried out by using specific antibodies against SGK1, AKT, MBP, and tubulin. DMSO, dimethyl sulfoxide.

under the same experimental conditions (Fig. 3A). Moreover, if the effect of SGK1 on MT depolymerization is physiological, a dose-dependent effect would be observed. We carried out a dose-response experiment to examine this issue. As revealed from Fig. 3B, in the absence of ATP, when the concentration of ΔN-SGK1 is increased (to 0.07, 0.2, and 0.4 μM), the MT

depolymerization effect is also increased. ΔN-SGK1 almost completely depolymerized self-polymerized MT at a concentration of 0.4 μM. A previous study has shown that pretreatment with dexamethasone, which upregulates SGK1, inhibits the therapeutic effect of paclitaxel (Taxol) on breast cancer through unknown mechanisms (59). Because Taxol is known to

enhance MT polymerization and stabilize MTs (24, 25), in this experiment, we further examined whether SGK1 disassembles Taxol-induced prepolymerized MT and whether this effect is also ATP independent. Similarly, AKT and MBP were used to examine the specificity of SGK1. A low concentration of tubulin (16 µM) was first treated with Taxol (25 µM). The Taxol-stabilized MT was then incubated with equal molars (0.2 µM) of ΔN-SGK1, AKT, and MBP in the absence of ATP. In this MT sedimentation experiment, polymerized MT is sedimented in the pellet fraction. However, when MT is depolymerized, free tubulin is released to the supernatant fraction and is no longer observed in the pellet fraction. The results revealed that Taxol effectively enhanced MT polymerization, but this effect is almost completely abolished by the addition of ΔN-SGK1 (Fig. 3C). Moreover, the addition of AKT or MBP did not destabilize Taxol-induced MT polymerization (Fig. 3C).

**SGK1 inhibits MT reassembly in vivo.** After establishing the effect of SGK1 on MT depolymerization in vitro, we further examined whether SGK1 affects MT assembly in vivo. EGFP-tagged fragments of human *sgk1* were transfected to HeLa cells for 24 h. The results revealed that the transfection of human FL *sgk1*, ΔN-*sgk1*, ΔC-*sgk1*, and the cat. domain *sgk1* all significantly inhibited MT reassembly from cold treatment in HeLa cells (Fig. 4). FL *sgk1*-transfected cells showed fewer and simpler MT bundles than vector-transfected cells. In ΔN-SGK1-, ΔC-SGK1-, and cat. domain SGK1-expressing cells, MT is bundled and curved at cell margins. ΔC-SGK1- and cat. domain-SGK1-expressing cells also showed various punctates and different distributions of SGK1. Little inhibition of MT reassembly was observed in cells transfected with C-terminal-only *sgk1*. Together, these results suggest that the same SGK1 fragments not only depolymerized MT in vitro but also prevented MT assembly in vivo.

**SGK1 is a tau protein kinase.** We have shown that SGK1 is associated with tau in cultured hippocampal neurons (Fig. 1I and J). Because tau plays an important role in MT stabilization (54) and also contains the sequence of the SGK1/AKT substrate motif (R-X-R-X-X-S/T-Ø; [Ø stands for hydrophobic amino acid]), we suspected that SGK1 may also affect MT stabilization through the phosphorylation of tau. To test this hypothesis, we first examined whether SGK1 is a candidate tau protein kinase. Active SGK1 was used to phosphorylate purified human full-length tau in vitro. To mimic the effect of active SGK1, Ser422 of N-terminally truncated SGK1 was mutated to Asp and is activated with 3-phosphoinositide-dependent protein kinase-1, a downstream signaling molecule of PI3K (16, 30). Results from an in vitro kinase assay revealed that the incubation of purified full-length tau (441 aa; 1 µg) with active SGK1 (100 ng) in the presence of [$\gamma$-$^{32}$P]ATP leads to detectable phosphate incorporation within 10 min (Fig. 5A). Degraded tau is observed at a molecular mass of around 50 to 58 kDa. By using a set of anti-phospho-tau Abs (pThr181, pSer202, pThr205, pThr212, pSer214, pThr231, pSer262, pSer396, pSer404, pSer409, and pSer422), we have found that only Ser214 of tau (R-S-R-T-P-S$_{214}$-L) is specifically phosphorylated by active SGK1 (Fig. 5B, left panel). This result fits perfectly with the SGK1/AKT substrate motif and is also consistent with the result of a recent report (10). A phosphorylation signal was not detected by using other site-specific phospho-tau Abs (data not shown). To further verify that tau is
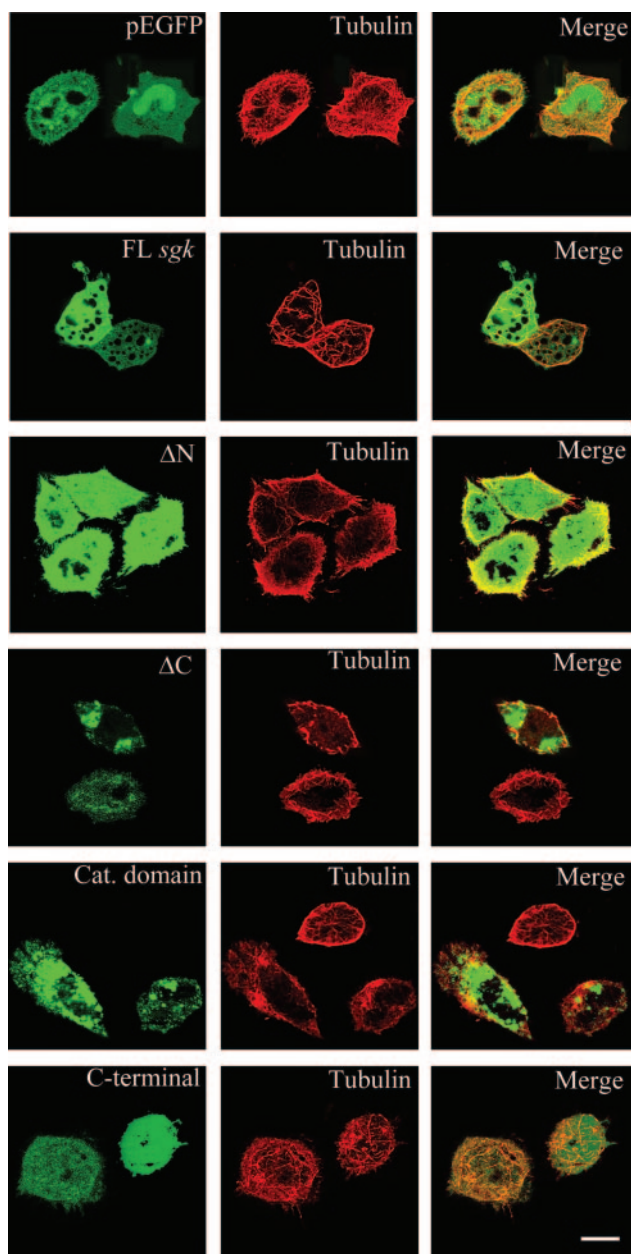


FIG. 4. SGK1 and its derived fragments inhibit MT reassembly from cold-treated HeLa cells. (A) HeLa cells were transiently transfected with pEGFP, pEGFP-FL-h*sgk1*, pEGFP-ΔN-h*sgk1*, pEGFP-ΔC-h*sgk1*, pEGFP-cat. domain-h*sgk1*, and pEGFP-C terminal-h*sgk1*. Twenty-four hours after transfection, the cells were cold treated (4°C) for 1 h to disassemble MT and then shifted to 37°C to reassemble MT. Cells were then fixed and stained with anti-β tubulin Ab (red). The EGFP-SGK1 fusion proteins are readily observed with a confocal fluorescence microscope. Scale bar, 40 µm.

phosphorylated by active SGK1 specifically at Ser214, Ser214 of tau was mutated to Ala and an in vitro kinase assay was carried out. The results revealed that, when Ser214 was mutated to Ala, active SGK1 no longer phosphorylates tau (Fig. 5B, right panel). To confirm the results obtained in vitro, we then cotransfected various *sgk1* and *tau* plasmids to HEK293T cells to assess the SGK1 phosphorylation of tau in vivo. Im-

FIG. 5. Tau, a microtubule-associated protein, is a substrate for SGK1. (A) *E. coli*-purified, His-tagged human tau 40 was incubated with an active form of SGK1 (a-SGK) in kinase buffer containing [γ-³²P]ATP for 10 min at 30°C. Half of the reaction mixture was subjected to 8% SDS-PAGE. Autoradiography showed that purified tau is highly phosphorylated by active SGK1 (left panel). The polyvinylidene difluoride (PVDF) membrane was reprobed with anti-tau Ab (right panel). WB, Western blot. (B) Among a set of anti-phospho-tau Abs (pThr181, pSer202, pThr205, pThr212, pSer214, pThr231, pSer262, pSer396, pSer404, pSer409, and pSer422) examined, only Ser214 of tau is specifically phosphorylated by active SGK1 (a-SGK) (left panel). PCR site-directed mutagenesis was conducted to generate

munoblotting results revealed that the highest phosphorylation level of tau Ser214 was observed when the constitutively active *sgk1* construct (HA-ΔN *sgk1*S422D) was transfected (Fig. 5C, compare lane 9 with lanes 7 and 8). However, when *tau* was replaced with *tau*S214A, SGK1 no longer phosphorylated tau (Fig. 5C, lanes 10 through 12). Together, these results suggest that SGK1 is a tau protein kinase and that SGK1 phosphorylates tau specifically at Ser214.

**SGK1 specifically phosphorylates Ser214 of tau in hippocampal neurons.** After confirming that SGK1 phosphorylates tau at Ser214 both in vitro and in HEK293T cells, we further examined whether SGK1 also phosphorylates tau in cultured hippocampal neurons. Endogenous tau from hippocampal tissue was immunoprecipitated with anti-tau-protein G–Sepharose cross-linked Ab, and active SGK1 was added to the immunoprecipitated product. The results revealed that active SGK1 increased the phosphorylation of endogenous tau (Fig. 6A). Immunoblotting results revealed that active SGK1 increased the level of phospho-tau Ser214 in a dose-dependent manner (Fig. 6B), but other phosphorylation sites (pThr181, pSer202, pThr205, pThr212, pThr231, pSer262, pSer396, pSer404, pSer409, and pSer422) of tau remained unchanged. pThr231 and pSer404 of tau were illustrated here as representative examples (Fig. 6B). In addition, a low basal level of phospho-tau Ser214 was observed, suggesting that tau Ser214 phosphorylation is highly regulated by external stimuli. To further examine whether SGK1 phosphorylates tau at Ser214 in hippocampal neurons in vivo, pEGFP or pEGFP-*sgk1* wild-type plasmid was transfected to cultured hippocampal neurons, followed by fluorescence-activated cell sorter (FACS) collection 24 h later, and subjected to immunoblot analysis. The results revealed that pEGFP-*sgk1* wild-type transfection increased the level of phospho-tau Ser214 in hippocampal neurons, but the protein levels of tau, tubulin, and actin remained unchanged (Fig. 6C, left panel). On the other hand, knocking down endogenous SGK1 by pSUPER-*sgk1* shRNA transfection significantly decreased the level of phospho-tau Ser214 (Fig. 6C, right panel). Similarly, the protein levels of tau, tubulin, and actin were not changed. If SGK1 phosphorylates endogenous tau in hippocampal neurons, SGK1 should be associated with tau and this association should be reduced if the level of endogenous SGK1 is decreased. We examined this issue by carrying out immunoprecipitation and immunoblotting experiments. The results revealed that tau was associated with SGK1 when the pSUPER vector was transfected to cultured hippocampal neurons. However, this association was decreased when hippocampal neurons were transfected with pSUPER-*sgk1* shRNA (Fig. 6D). Due to the limitation of the
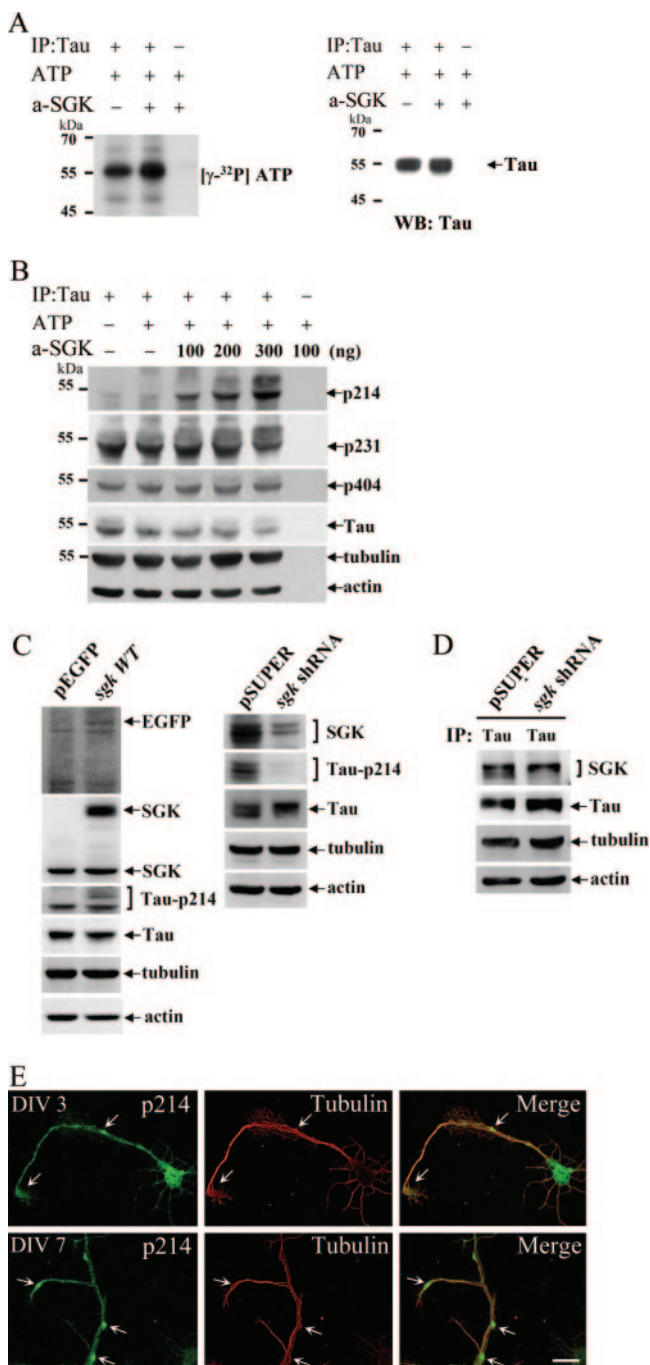
FIG. 6. SGK1 specifically phosphorylates tau at Ser214 in hippocampal neurons. Endogenous tau was immunoprecipitated (IP) by the incubation of anti-tau-protein G–Sepharose cross-linked Ab with 1,500 μg rat hippocampal lysate and was divided into five aliquots for a subsequent kinase assay. (A) An aliquot of immunoprecipitated tau was incubated with active SGK1 in kinase buffer containing [γ-$^{32}$P]ATP for 10 min at 30°C and was subjected to 8% SDS-PAGE. Autoradiography showed that the phosphorylation of endogenous tau is increased immediately after an incubation with active SGK1 (a-SGK) (left panel). The polyvinylidene difluoride membrane was reprobed with monoclonal anti-tau Ab (right panel). WB, Western blot. −, absence of; +, presence of. (B) Active SGK1 (a-SGK) (100, 200, and 300 ng) was incubated with immunoprecipitated tau aliquots for 10 min at 30°C. Half of the reaction mixture was subjected to 8% SDS-PAGE. Immunoblotting was performed with Abs specific for tau-

availability of Ab species for SGK and phopho-tau Ser214, immunostaining of endogenous SGK and phospho-tau Ser214 cannot be performed at the same time. Nevertheless, in our observations, the distribution of endogenous phospho-tau Ser214 where MT is not bundled (Fig. 6E) is similar to that of SGK1 (Fig. 1H).

**SGK1 depolymerizes MTs through the phosphorylation of tau at Ser214 in vitro.** Because tau is important for MT stabilization, we next examined whether SGK1 may affect MT polymerization through the phosphorylation of tau. An in vitro MT polymerization assay was carried out to test this hypothesis. Results shown in Fig. 7 revealed that once purified full-length tau (3.8 μM) was added to a low concentration of tubulin (35 μM), MT polymerization proceeded immediately (Fig. 7A). So did TauS214A (Fig. 7A). However, when tau was first phosphorylated by active SGK1, it no longer promoted MT polymerization (Fig. 7B). On the other hand, when purified TauS214A was incubated with active SGK1, MT polymerization proceeded to the end of the experiment (Fig. 7A). To further confirm that MT polymerization is blocked by SGK1 phosphorylation of tau, immunostaining was carried out after spectrophotometric recording. As shown in Fig. 7B, MT polymerization was promoted by unphosphorylated tau (upper middle panel), indicating that the recombinant human full-length tau is biologically functional. In contrast, dotted precipitant, which stands for depolymerized MT, was observed when SGK1-phosphorylated tau was added (lower middle panel). Similarly, TauS214A prevented the effect of active SGK1 on MT depolymerization (lower right panel). In addition, the inhibition of MT polymerization was observed when active SGK1 alone was introduced (Fig. 7B, lower left panel). This result is consistent with our above observation that SGK1 directly depolymerized MT in vitro (Fig. 2).

**SGK1 increases neurite formation through the phosphorylation of tau at Ser214 in hippocampal neurons.** The above results demonstrated that SGK1 inhibited MT polymerization through the phosphorylation of tau at Ser214 in vitro. In this experiment, we examined whether SGK1 phosphorylation of tau mediates hippocampal neurite formation. Plasmids, includ-

---

pSer214, tau-pSer231, tau-pSer404, tau, tubulin, and actin. −, absence of; +, presence of. (C) Ser214 of tau is phosphorylated by SGK1 in hippocampal neurons. pEGFP, pEGFP-*sgk1*WT, pSUPER, and pSUPER-*sgk1* shRNA plasmids were transfected to hippocampal neurons at DIV 0. Twenty-four hours later, pEGFP- and pEGFP-*sgk1*WT-transfected neurons were collected by FACS (left panel). To obtain a better effect of knocking down SGK1, pSUPER- and pSUPER-*sgk1* shRNA-transfected neurons were collected by FACS 48 h after transfection (right panel). The collected neurons were lysed, extracted, and subjected to 8% SDS-PAGE. Immunoblotting was performed with Abs specific for EGFP, SGK1, tau-pSer214, tau, tubulin, and actin. (D) Tau is associated with SGK1 in hippocampal neurons, and this association is decreased in cells transfected with *sgk1* shRNA. As described for panel C, tau was immunoprecipitated (IP) from hippocampal lysate and subjected to 8% SDS-PAGE. Immunoblotting was performed with Abs specific for SGK1, tau, tubulin, and actin. (E) Confocal images showed the double staining results of phospho-tau Ser214 and tubulin. Phospho-tau Ser214 (green) is distributed in a punctate pattern and concentrated at regions devoid of stabilized MT (red) (arrows and green color). Upper panels show DIV 3, and lower panels show DIV 7. Scale bar, 20 μm.
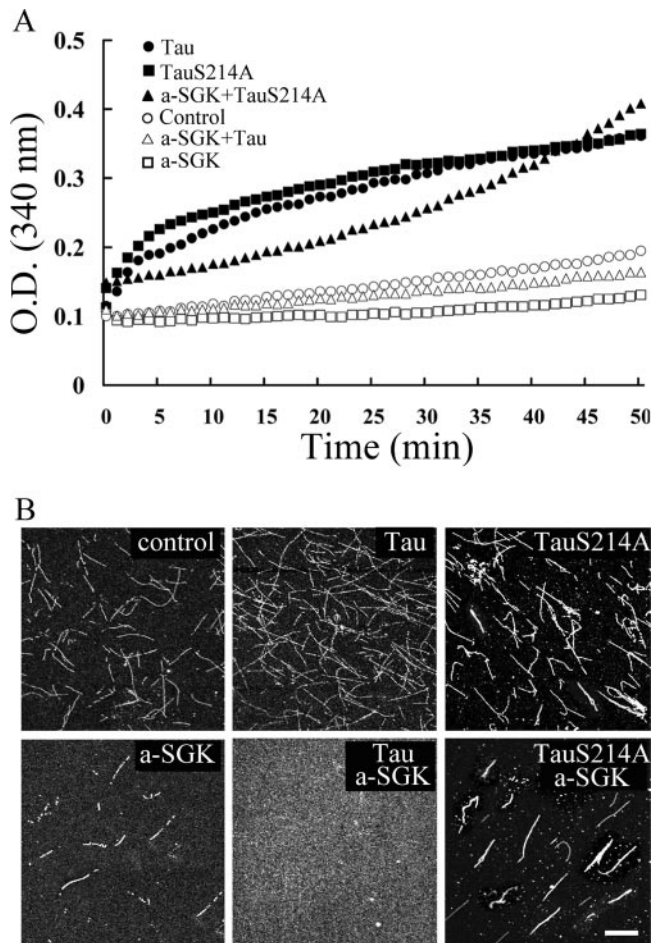
FIG. 7. SGK1 inhibits MT polymerization through the phosphory-lation of tau at Ser214. The low concentration of bovine brain-purified tubulin used here requires MAP, like tau, to promote MT polymer-ization. (A) In vitro MT polymerization was continuously recorded at 37°C by spectrophotometry at an absorbance of 340 nm. *E. coli*-puri-fied, human full-length tau and TauS214A both induced MT polymer-ization. When tau was first phosphorylated by active SGK1 (a-SGK1) for 10 min at 30°C, MT polymerization no longer took place. However, MT polymerization continued when active SGK1 was incubated with TauS214A. As noticed, active SGK1 alone also caused a slight inhibi-tion of MT polymerization compared with that of the control tubulin group. (B) The reaction mixture used for panel A was ultracentrifuged to coverslips and immunostained with anti-β III tubulin Ab after 50 min of spectrophotometric recording. The confocal images showed that both the length and density of MT were increased in the presence of tau and TauS214A. But when tau was phosphorylated by active SGK1, MT severely broke into sparse dots on the coverslip. However, when TauS214A was incubated with active SGK1, MT bundles were still observed. Scale bar, 40 μm. a-SGK1, active SGK1.
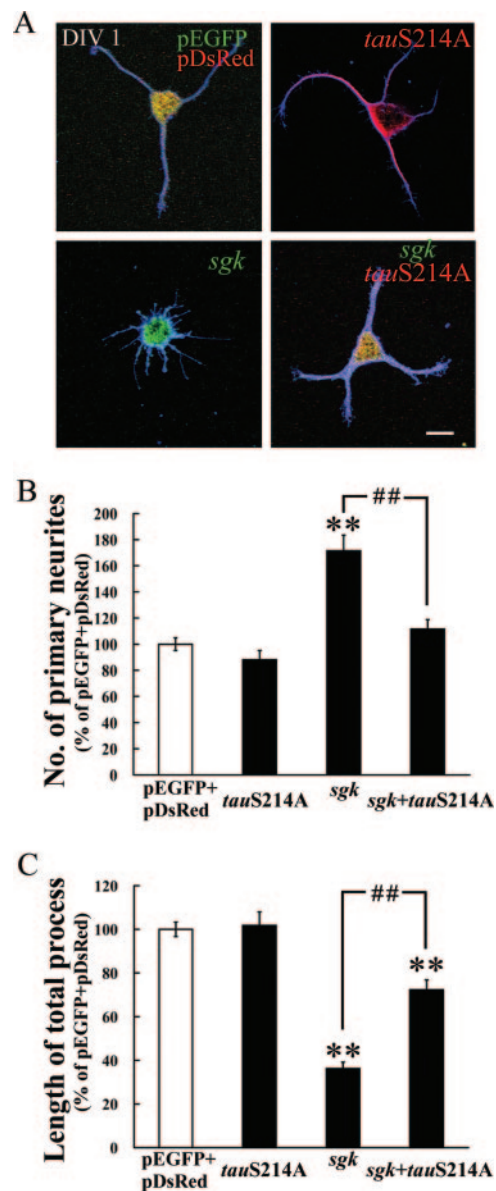


FIG. 8. SGK1 increases hippocampal neurite formation through the phosphorylation of tau at Ser214. (A) pEGFP-*sgk1* (green), pDsRed-*tau*S214A (red) or the combination of pEGFP-*sgk1* and pDsRed-*tau*S214A was transfected to dissociated hippocampal neurons at DIV 0 and fixed at DIV 1. Neuronal processes were visualized by immuno-staining with anti-β III tubulin Ab (blue). The EGFP-SGK1 and DsRed-TauS214A fusion proteins were readily observed with a con-focal fluorescence microscope. Scale bar, 10 μm. (B) The transfection of *sgk1* markedly increased the number of primary neurites, and this effect was reversed by the cotransfection of *tau*S214A. (C) The trans-fection of *sgk1* also decreased the length of the total process, and this effect was antagonized by the cotransfection of *tau*S214A. $n = 70, 64, 44,$ and 69 for vector, pDsRed-*tau*S214A, pEGFP-*sgk1* and pEGFP-*sgk1*+pDsRed-*tau*S214A groups, respectively. Data are expressed as means ± standard errors of the means (error bars). ∗∗, $P$ was $<0.01$ as determined by one-way analysis of variance, followed by Dunnett's $t$ test, compared with that of the vector transfection group; # #, $P$ was $<0.01$, as determined by one-way analysis of variance, followed by Newman-Keuls statistics, compared with that of the *sgk1* transfection group.

ing pEGFP-*sgk1*, pDsRed-*tau*S214A, or the combination of pEGFP-*sgk1* and pDsRed-*tau*S214A, were transfected to cul-tured hippocampal neurons at DIV 0, and their effects on neurite formation were examined 24 h later. The results re-vealed that pEGFP-*sgk1* transfection markedly increased the number of primary neurites (Dunnett's $t$ test [$tD$] $= 6.7; P <$ 0.01) and decreased the length of the total neurite process ($tD = 8.8; P < 0.01$) in hippocampal neurons (Fig. 8). Both effects were significantly reversed by the cotransfection of the
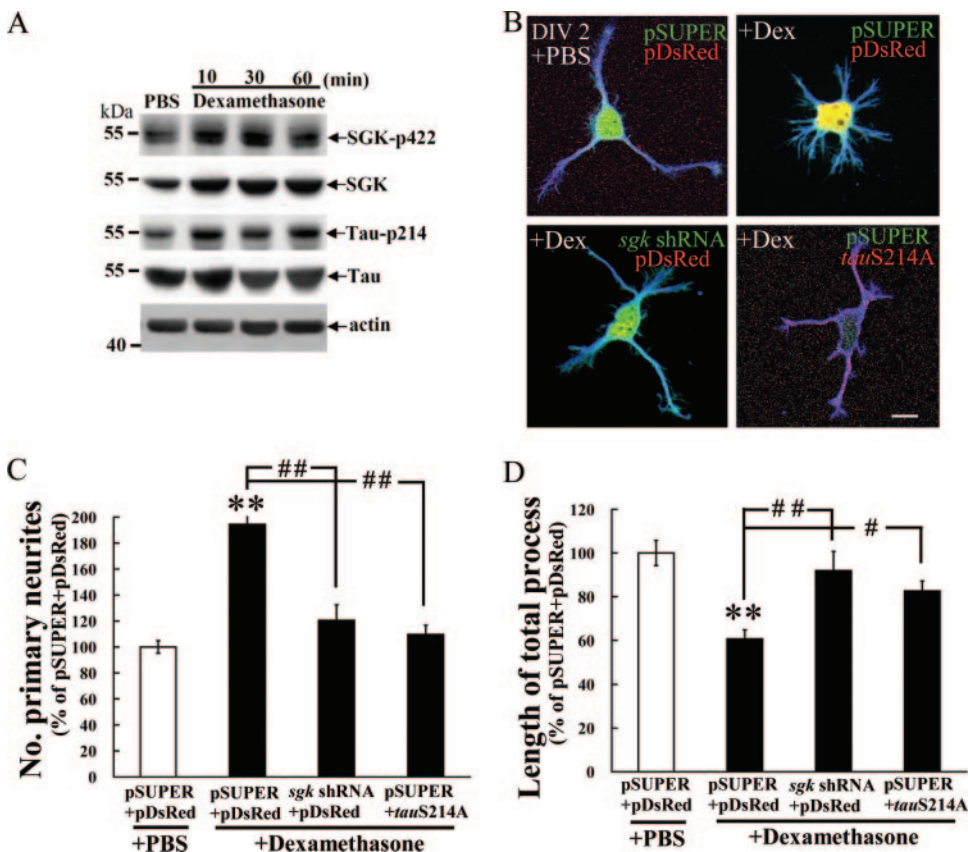
FIG. 9. SGK1 and tau Ser214 phosphorylation mediate the effects of dexamethasone on hippocampal neurite formation. (A) Cultured hippocampal neurons were treated with 1 μM dexamethasone, and Western blotting for SGK1, pSGK1 Ser422, pTau Ser214, tau, and β-actin was carried out. Dexamethasone increased the protein levels of SGK1, pSGK1 Ser422, and pTau Ser214 at 10 min, 30 min, and 1 h after treatment. (B) sgk1 shRNA or tauS214A was transfected to cultured hippocampal neurons as described above to examine its influence on the effect of dexamethasone on neurite formation. Dexamethasone markedly enhanced hippocampal neurite formation, as indicated by a significant increase in the number of primary neurites (C) and a significant shortening in the length of the total process (D). This effect was blocked by prior transfection of sgk1 shRNA and tauS214A mutant plasmid. Scale bar, 10 μm. n = 37, 37, 12, and 14 for the pSUPER+pDsRed+phosphate-buffered saline (PBS), pSUPER+pDsRed+dexamethasone, sgk1 shRNA+pDsRed+dexamethasone and pSUPER+tauS214A+dexamethasone groups, respectively. Data are expressed as means ± standard errors of the means (error bars). Statistics are expressed as for Fig. 8. #, $P < 0.05$; # #, $P < 0.01$.

pDsRed-tauS214A plasmid (q [Newman-Kuels statistics] was 59.8 and 36.1, both with P values of <0.01 compared with the those of the pEGFP-sgk1 group). However, the cotransfection of pDsRed-tauS214A did not completely prevent the effect of pEGFP-sgk1 on process shortening (approximately 75% of the control group). This is probably because the direct MT depolymerization caused by pEGFP-sgk1 transfection contributes to part of the effect. Because MT destabilization is an important mechanism for neurite outgrowth (12, 17, 50), together, these results suggest that pEGFP-sgk1-induced neurite plasticity is mediated through SGK1 phosphorylation of tau at Ser214.

SGK1 and tau Ser214 phosphorylation mediate the effect of dexamethasone on hippocampal neurite formation. The above results demonstrated that the overexpression of SGK1 increased neurite formation through the phosphorylation of tau at Ser214. However, these results do not reveal whether the endogenous elevation of SGK1 also increases neurite formation and whether this effect is mediated through tau Ser214 phosphorylation. The present experiment was aimed to address this issue. Dexamethasone, a synthetic glucocor-

ticoid, was applied to cultured hippocampal neurons because SGK1 was shown to be transcriptionally regulated mainly by glucocorticoid (57). In other groups of cells, sgk1 shRNA or tauS214A was transfected to examine whether it alters the effect of dexamethasone on neurite formation. The results revealed that dexamethasone (1 μM) increased SGK1 and phospho-SGK1 Ser422 protein levels at 10 min, 30 min, and 1 h later (Fig. 9A). It also increased the level of phospho-tau Ser214 at the same time points (Fig. 9A). Meanwhile, dexamethasone significantly enhanced hippocampal neurite formation (Fig. 9B), as indicated by a marked increase in the number of primary neurites ($tD = 6.9$; $P < 0.01$) (Fig. 9C) and a decrease in the length of the total process ($tD = 6.1$, $P < 0.01$) (Fig. 9D), presumably due to MT depolymerization. However, these effects of dexamethasone were abolished by the transfection of sgk1 shRNA and tauS214A mutant plasmid (P values were <0.01 or <0.05 compared with that of the corresponding dexamethasone group) (Fig. 9B through D). These results suggest that the effect of dexamethasone on neurite formation

is mediated through SGK1 expression and tau Ser214 phosphorylation in hippocampal neurons.

## DISCUSSION

In the present study, we have found that the overexpression of SGK1 in cultured hippocampal neurons significantly increases the number of primary neurites. This result is consistent with that of a recent report showing that the transfection of constitutively active *sgk1* enhances dendritic growth and dendritic branching in cultured spinal cord neurons (11). We hypothesized that this effect is probably due to MT depolymerization caused by SGK1 because MT dynamic instability plays an important role in process formation (12, 17, 50). In addressing this issue, we have found two novel mechanisms of SGK1 in the depolymerization MT. First, SGK1 directly depolymerizes MT and this effect is independent of its kinase activity. We found that ΔN-*sgk1*, FL *sgk1*, cat. domain *sgk1* and ΔC-*sgk1* all effectively depolymerized MT. Although no conserved MT-binding domain was found in SGK1, SGK1 may interact with MT via other atypical domains, such as in the cases of CPAP (centrosomal protein 4.1-associated protein) and casein kinase II. CPAP, a centrosomal protein, carries a novel MT-destabilizing motif that inhibits MT nucleation from the centrosome and depolymerizes Taxol-stabilized MT (25). Another example is casein kinase II. Casein kinase II also acts as an MT stabilizer in an ATP-independent manner through an unknown MT-binding domain (37). Then what might be the mechanism for SGK1 depolymerization of MT? Several models have been proposed for certain MT destabilizers, such as the catastrophe model for kin I kinesin (14), the catastrophe and sequestering models for stathmin (4, 29), the severing model for katanin and spastin (21, 51), and the capping, sequestering, and severing models for CPAP (25). In the present study, SGK1 disassembled self-polymerized MT into fragments and dotted precipitants at higher concentrations both in vitro and in vivo. This result resembles those found with spastin and katanin (51, 62). Thus, SGK1 may share similar mechanisms with spastin and katanin. In addition, SGK1 could effectively block MT assembly at a 1:100 molar concentration ratio to tubulin. SGK1 also prevents new MT assembly after a temperature shift. This result suggests that SGK1 may depolymerize MT through capping the plus end of MT or inhibiting MT nucleation or through the severing model. The exact mechanism for SGK1 depolymerization of MT requires further investigation.

Second, SGK1 depolymerizes MT through phosphorylation of tau at Ser214. Many protein kinases are known to phosphorylate tau either at the proline-directed SP/TP motif or at the KXGS motif, and the phosphorylation sites on these motifs are known epitopes for an Ab diagnosis of Alzheimer's disease (28). In the present study, SGK1 was found to phosphorylate tau at a non-proline-directed site, Ser214 (R-S-R-T-P-S$_{214}$-L). This result is consistent with that of the report stating that SGK1 phosphorylates Ser214 of tau in vitro (10). But we have extended this finding by showing that SGK1 phosphorylation of tau Ser214 mediates MT depolymerization and neurite formation in hippocampal neurons. Although the repeat domain of tau constitutes the MT-binding sites, a sequence containing Ser214 adjacent to the repeat domain was found to be necessary for tau binding to MT in cells and it also contributes to

profound MT bundling (20, 35). Then what is the role of tau Ser214 phosphorylation in the cell? In CHO cells, tau Ser214 phosphorylation is increased when cells enter mitosis (26), a stage that requires MT disassembly (40). Further, Ser214 is one of the protein kinase A phosphorylation sites and when protein kinase A phosphorylates tau, tau is detached from MT and consequently causes in vitro MT depolymerization (26). These results are consistent with our finding that SGK1 phosphorylates Ser214 of tau to cause MT depolymerization. Moreover, when tau Ser214 was first phosphorylated, the neighboring sites were resistant to further proline-directed phosphorylation (63) and against the aggregation of tau into a paired helical filament (53). These results suggest that SGK1 phosphorylation of tau is probably not related to the pathogenesis of Alzheimer's disease. In addition, the transfection of *tau*S214A did not completely reverse the effects of *sgk1* and dexamethasone on total process shortening (approximately 75 and 80%, respectively, of control) (Fig. 8C and 9D). This is probably because the direct MT depolymerization caused by SGK1 contributes to part of the effect (Fig. 2). However, other possibilities cannot be ruled out. For example, SGK1 may affect MT stability through acting on MAP2 because MAP2 is a dendritic MAP (18) and it also carries the SGK1/AKT substrate motif. SGK1 may also affect MT polymerization through the activation of glycogen synthase kinase 3β (GSK-3β) because GSK-3β was shown to regulate MT assembly (19). In another study, the transfection of active *akt* was similarly found to increase the branching of sensory neurons (42). However, although SGK1 and AKT share 45 to 55% homology in their catalytic domains, the mechanisms for SGK1 and AKT to increase neuronal branching may be different because SGK1 was found to directly inhibit MT polymerization in the present study, whereas AKT was not. Moreover, AKT prefers Thr212 rather than Ser214 of tau when AKT phosphorylates tau (31).

In addition to disassembling self-polymerized MT, SGK1 also disassembled prepolymerized MT induced by Taxol. Taxol was shown to inhibit cancer cell mitosis through MT stabilization, and dexamethasone was shown to inhibit the chemotherapeutic effect of Taxol through unknown mechanisms (59). Since dexamethasone is a synthetic glucocorticoid that enhances *sgk1* transcription, our results suggest that dexamethasone may antagonize the effect of Taxol through MT destabilization caused by increased SGK1 expression.

Then what are the upstream signals of SGK1 that affect MT polymerization? Glucocorticoid has been shown to induce hippocampal structural changes (43, 52). Because *sgk1* is transcriptionally regulated mainly by glucocorticoid (57), glucocorticoid could be an upstream signal of SGK1 regulating MT dynamics. This suggestion is supported by the present finding that dexamethasone enhanced hippocampal neurite formation, and this effect is blocked by prior *sgk1* shRNA transfection and *tau*S214A mutant plasmid transfection. These results also indicate that endogenous SGK expression regulates MT polymerization through the phosphorylation of tau at Ser214. On the other hand, PI3K signaling was shown to mediate nerve growth factor- and brain-derived neurotrophic factor-induced neurite formation in primary neurons (15, 61, 64). SGK1 is a downstream target of PI3K-3-phosphoinositide-dependent protein kinase-1 signaling (30, 48). Therefore, PI3K may be another upstream signal of SGK that regulates MT polymer-

ization. More recently, SGK1 was shown to be phosphorylated by mitogen-activated protein kinase/extracellular signal-regulated kinase (MAPK/ERK) (32) and MAPK/ERK was shown to mediate the effect of brain-derived neurotrophic factor in increasing the dendritic spines of hippocampal neurons (2). Further, MAPK/ERK was shown to transcriptionally regulate *sgk1* expression (46). These results suggest that MAPK/ERK could be another upstream signal of SGK1 that regulates MT stability. Taken together, our results suggest that SGK1 increases hippocampal neurite formation through MT depolymerization. This is achieved by SGK1 depolymerization of MT directly and by SGK1 phosphorylation of tau at Ser214.

## ACKNOWLEDGMENTS

## REFERENCES

1. **Ahmad, F. J., W. Yu, F. J. McNally, and P. W. Baas.** 1999. An essential role for katanin in severing microtubules in the neuron. J. Cell Biol. **145:**305–315.
2. **Alonso, M., J. H. Medina, and L. Pozzo-Miller.** 2004. ERK1/2 activation is necessary for BDNF to increase dendritic spine density in hippocampal CA1 pyramidal neurons. Learn. Mem. **11:**172–178.
3. **Avila, J., J. Dominguez, and J. Diaz-Nido.** 1994. Regulation of microtubule dynamics by microtubule-associated protein expression and phosphorylation during neuronal development. Int. J. Dev. Biol. **38:**13–25.
4. **Belmont, L. D., and T. J. Mitchison.** 1996. Identification of a protein that interacts with tubulin dimers and increases the catastrophe rate of microtubules. Cell **84:**623–631.
5. **Brummelkamp, T. R., R. Bernards, and R. Agami.** 2002. A system for stable expression of short interfering RNAs in mammalian cells. Science **296:**550–553.
6. **Buse, P., S. H. Tran, E. Luther, P. T. Phu, G. W. Aponte, and G. L. Firestone.** 1999. Cell cycle and hormonal control of nuclear-cytoplasmic localization of the serum- and glucocorticoid-inducible protein kinase, Sgk, in mammary tumor cells. A novel convergence point of anti-proliferative and proliferative cell signaling pathways. J. Biol. Chem. **274:**7253–7263.
7. **Caceres, A., S. Potrebic, and K. S. Kosik.** 1991. The effect of tau antisense oligonucleotides on neurite formation of cultured cerebellar macroneurons. J. Neurosci. **11:**1515–1523.
8. **Cassimeris, L.** 1993. Regulation of microtubule dynamic instability. Cell Motil. Cytoskelet. **26:**275–281.
9. **Cassimeris, L., and C. Spittle.** 2001. Regulation of microtubule-associated proteins. Int. Rev. Cytol. **210:**163–226.
10. **Chun, J., T. Kwon, E. J. Lee, C. H. Kim, Y. S. Han, S. K. Hong, S. Hyun, and S. S. Kang.** 2004. 14-3-3 Protein mediates phosphorylation of microtubule-associated protein tau by serum- and glucocorticoid-induced protein kinase 1. Mol. Cells **18:**360–368.
11. **David, S., S. L. Stegenga, P. Hu, G. Xiong, E. Kerr, K. B. Becker, S. Venkatapathy, J. A. Warrington, and R. G. Kalb.** 2005. Expression of serum- and glucocorticoid-inducible kinase is regulated in an experience-dependent manner and can cause dendrite growth. J. Neurosci. **25:**7048–7053.
12. **Dent, E. W., and F. B. Gertler.** 2003. Cytoskeletal dynamics and transport in growth cone motility and axon guidance. Neuron **40:**209–227.
13. **Desai, A., S. Verma, T. J. Mitchison, and C. E. Walczak.** 1999. Kin I kinesins are microtubule-destabilizing enzymes. Cell **96:**69–78.
14. **de Silva, R., and M. Farrer.** 2002. Tau neurotoxicity without the lesions: a fly challenges a tangled web. Trends Neurosci. **25:**327–329.
15. **Dijkhuizen, P. A., and A. Ghosh.** 2005. BDNF regulates primary dendrite formation in cortical neurons via the PI3-kinase and MAP kinase signaling pathways. J. Neurobiol. **62:**278–288.
16. **Firestone, G. L., J. R. Giampaolo, and B. A. O'Keeffe.** 2003. Stimulus-dependent regulation of serum and glucocorticoid inducible protein kinase (SGK) transcription, subcellular localization and enzymatic activity. Cell. Physiol. Biochem. **13:**1–12.
17. **Gao, P. P., Y. Yue, D. P. Cerretti, C. Dreyfus, and R. Zhou.** 1999. Ephrin-dependent growth and pruning of hippocampal axons. Proc. Natl. Acad. Sci. USA **96:**4073–4077.
18. **Goedert, M., R. A. Crowther, and C. C. Garner.** 1991. Molecular characterization of microtubule-associated proteins tau and MAP2. Trends Neurosci. **14:**193–199.
19. **Goold, R. G., R. Owen, and P. R. Gordon-Weeks.** 1999. Glycogen synthase kinase 3β phosphorylation of microtubule-associated protein 1B regulates the stability of microtubules in growth cones. J. Cell Sci. **112:**3373–3384.
20. **Gustke, N., B. Trinczek, J. Biernat, E. M. Mandelkow, and E. Mandelkow.** 1994. Domains of tau protein and interactions with microtubules. Biochemistry **33:**9511–9522.
21. **Hartman, J. J., and R. D. Vale.** 1999. Microtubule disassembly by ATP-dependent oligomerization of the AAA enzyme katanin. Science **286:**782–785.
22. **Heald, R., and E. Nogales.** 2002. Microtubule dynamics. J. Cell Sci. **115:**3–4.
23. **Hill, C. M., D. S. Libich, and G. Harauz.** 2005. Assembly of tubulin by classic myelin basic protein isoforms and regulation by post-translational modification. Biochemistry **44:**16672–16683.
24. **Horwitz, S. B.** 1994. Taxol (paclitaxel): mechanisms of action. Ann. Oncol. **5**(Suppl 6):S3–S6.
25. **Hung, L. Y., H. L. Chen, C. W. Chang, B. R. Li, and T. K. Tang.** 2004. Identification of a novel microtubule-destabilizing motif in CPAP that binds to tubulin heterodimers and inhibits microtubule assembly. Mol. Biol. Cell **15:**2697–2706.
26. **Illenberger, S., Q. Zheng-Fischhofer, U. Preuss, K. Stamer, K. Baumann, B. Trinczek, J. Biernat, R. Godemann, E. M. Mandelkow, and E. Mandelkow.** 1998. The endogenous and cell cycle-dependent phosphorylation of tau protein in living cells: implications for Alzheimer's disease. Mol. Biol. Cell **9:**1495–1512.
27. **Inoue, S., and E. D. Salmon.** 1995. Force generation by microtubule assembly/disassembly in mitosis and related movements. Mol. Biol. Cell **6:**1619–1640.
28. **Johnson, G. V., and W. H. Stoothoff.** 2004. Tau phosphorylation in neuronal cell function and dysfunction. J. Cell Sci. **117:**5721–5729.
29. **Jourdain, L., P. Curmi, A. Sobel, D. Pantaloni, and M. F. Carlier.** 1997. Stathmin: a tubulin-sequestering protein which forms a ternary T2S complex with two tubulin molecules. Biochemistry **36:**10817–10821.
30. **Kobayashi, T., and P. Cohen.** 1999. Activation of serum- and glucocorticoid-regulated protein kinase by agonists that activate phosphatidylinositol 3-kinase is mediated by 3-phosphoinositide-dependent protein kinase-1 (PDK1) and PDK2. Biochem. J. **339:**319–328.
31. **Ksiezak-Reding, H., H. K. Pyo, B. Feinstein, and G. M. Pasinetti.** 2003. Akt/PKB kinase phosphorylates separately Thr212 and Ser214 of tau protein in vitro. Biochim. Biophys. Acta **1639:**159–168.
32. **Lee, C. T., S. W. Tyan, Y. L. Ma, M. C. Tsai, Y. C. Yang, and E. H. Lee.** 2006. Serum- and glucocorticoid-inducible kinase (SGK) is a target of the MAPK/ERK signaling pathway that mediates memory formation in rats. Eur. J. Neurosci. **23:**1311–1320.
33. **Lee, E., E. S. Lein, and G. L. Firestone.** 2001. Tissue-specific expression of the transcriptionally regulated serum and glucocorticoid-inducible protein kinase (Sgk) during mouse embryogenesis. Mech. Dev. **103:**177–181.
34. **Lee, E. H., W. L. Hsu, Y. L. Ma, P. J. Lee, and C. C. Chao.** 2003. Enrichment enhances the expression of *sgk*, a glucocorticoid-induced gene, and facilitates spatial learning through glutamate AMPA receptor mediation. Eur. J. Neurosci. **18:**2842–2852.
35. **Lee, G., and S. L. Rook.** 1992. Expression of tau protein in non-neuronal cells: microtubule binding and stabilization. J. Cell Sci. **102:**227–237.
36. **Liedtke, W., E. E. Leman, R. E. Fyffe, C. S. Raine, and U. K. Schubart.** 2002. Stathmin-deficient mice develop an age-dependent axonopathy of the central and peripheral nervous systems. Am. J. Pathol. **160:**469–480.
37. **Lim, A. C., S. Y. Tiu, Q. Li, and R. Z. Qi.** 2004. Direct regulation of microtubule dynamics by protein kinase CK2. J. Biol. Chem. **279:**4433–4439.
38. **Lu, R., H. Wang, Z. Liang, L. Ku, T. O'Donnell, W. Li, S. T. Warren, and Y. Feng.** 2004. The fragile X protein controls microtubule-associated protein 1B translation and microtubule stability in brain neuron development. Proc. Natl. Acad. Sci. USA **101:**15201–15206.
39. **Ma, Y. L., M. C. Tsai, W. L. Hsu, and E. H. Lee.** 2006. SGK protein kinase facilitates the expression of long-term potentiation in hippocampal neurons. Learn. Mem. **13:**114–118.
40. **Maiato, H., P. Sampaio, and C. E. Sunkel.** 2004. Microtubule-associated proteins and their essential roles during mitosis. Int. Rev. Cytol. **241:**53–153.
41. **Maiyar, A. C., M. L. Leong, and G. L. Firestone.** 2003. Importin-alpha mediates the regulated nuclear targeting of serum- and glucocorticoid-inducible protein kinase (Sgk) by recognition of a nuclear localization signal in the kinase central domain. Mol. Biol. Cell **14:**1221–1239.
42. **Markus, A., J. Zhong, and W. D. Snider.** 2002. Raf and Akt mediate distinct aspects of sensory axon growth. Neuron **35:**65–76.
43. **McEwen, B. S.** 2005. Glucocorticoids, depression, and mood disorders: structural remodeling in the brain. Metabolism **54:**20–23.
44. **McNally, F. J., and R. D. Vale.** 1993. Identification of katanin, an ATPase that severs and disassembles stable microtubules. Cell **75:**419–429.
45. **Mershin, A., E. Pavlopoulos, O. Fitch, B. C. Braden, D. V. Nanopoulos, and E. M. Skoulakis.** 2004. Learning and memory deficits upon TAU accumulation in *Drosophila* mushroom body neurons. Learn. Mem. **11:**277–287.
46. **Mizuno, H., and E. Nishida.** 2001. The ERK MAP kinase pathway mediates induction of SGK (serum- and glucocorticoid-inducible kinase) by growth factors. Genes Cells **6:**261–268.

47. **Nakayama, T., and T. Sawada.** 2002. Involvement of microtubule integrity in memory impairment caused by colchicine. Pharmacol. Biochem. Behav. **71:** 119–138.

48. **Park, J., M. L. Leong, P. Buse, A. C. Maiyar, G. L. Firestone, and B. A. Hemmings.** 1999. Serum and glucocorticoid-inducible kinase (SGK) is a target of the PI 3-kinase-stimulated signaling pathway. EMBO J. **18:**3024–3033.

49. **Riederer, B. M., V. Pellier, B. Antonsson, G. Di Paolo, S. A. Stimpson, R. Lutjens, S. Catsicas, and G. Grenningloh.** 1997. Regulation of microtubule dynamics by the neuronal growth-associated protein SCG10. Proc. Natl. Acad. Sci. USA **94:**741–745.

50. **Rochlin, M. W., K. M. Wickline, and P. C. Bridgman.** 1996. Microtubule stability decreases axon elongation but not axoplasm production. J. Neurosci. **16:**3236–3246.

51. **Roll-Mecak, A., and R. D. Vale.** 2005. The *Drosophila* homologue of the hereditary spastic paraplegia protein, spastin, severs and disassembles microtubules. Curr. Biol. **15:**650–655.

52. **Sapolsky, R. M., H. Uno, C. S. Rebert, and C. E. Finch.** 1990. Hippocampal damage associated with prolonged glucocorticoid exposure in primates. J. Neurosci. **10:**2897–2902.

53. **Schneider, A., J. Biernat, M. von Bergen, E. Mandelkow, and E. M. Mandelkow.** 1999. Phosphorylation that detaches tau protein from microtubules (Ser262, Ser214) also protects it against aggregation into Alzheimer paired helical filaments. Biochemistry **38:**3549–3558.

54. **Stoothoff, W. H., and G. V. Johnson.** 2005. Tau phosphorylation: physiological and pathological consequences. Biochim. Biophys. Acta **1739:**280–297.

55. **Trotta, N., G. Orso, M. G. Rossetto, A. Daga, and K. Broadie.** 2004. The hereditary spastic paraplegia gene, spastin, regulates microtubule stability to modulate synaptic structure and function. Curr. Biol. **14:**1135–1147.

56. **Tsai, K. J., S. K. Chen, Y. L. Ma, W. L. Hsu, and E. H. Lee.** 2002. *sgk*, a primary glucocorticoid-induced gene, facilitates memory consolidation of spatial learning in rats. Proc. Natl. Acad. Sci. USA **99:**3990–3995.

57. **Webster, M. K., L. Goya, Y. Ge, A. C. Maiyar, and G. L. Firestone.** 1993. Characterization of *sgk*, a novel member of the serine/threonine protein kinase gene family which is transcriptionally induced by glucocorticoids and serum. Mol. Cell. Biol. **13:**2031–2040.

58. **Wheal, H. V., Y. Chen, J. Mitchell, M. Schachner, W. Maerz, H. Wieland, D. Van Rossum, and J. Kirsch.** 1998. Molecular mechanisms that underlie structural and functional changes at the postsynaptic membrane during synaptic plasticity. Prog. Neurobiol. **55:**611–640.

59. **Wu, W., S. Chaudhuri, D. R. Brickley, D. Pang, T. Karrison, and S. D. Conzen.** 2004. Microarray analysis reveals glucocorticoid-regulated survival genes that are associated with inhibition of apoptosis in breast epithelial cells. Cancer Res. **64:**1757–1764.

60. **Yang, Y. C., Y. L. Ma, S. K. Chen, C. W. Wang, and E. H. Lee.** 2003. Focal adhesion kinase is required, but not sufficient, for the induction of long-term potentiation in dentate gyrus neurons in vivo. J. Neurosci. **23:**4072–4080.

61. **Yoshimura, T., Y. Kawano, N. Arimura, S. Kawabata, A. Kikuchi, and K. Kaibuchi.** 2005. GSK-3beta regulates phosphorylation of CRMP-2 and neuronal polarity. Cell **120:**137–149.

62. **Yu, W., J. M. Solowska, L. Qiang, A. Karabay, D. Baird, and P. W. Baas.** 2005. Regulation of microtubule severing by katanin subunits during neuronal development. J. Neurosci. **25:**5573–5583.

63. **Zheng-Fischhofer, Q., J. Biernat, E. M. Mandelkow, S. Illenberger, R. Godemann, and E. Mandelkow.** 1998. Sequential phosphorylation of tau by glycogen synthase kinase-3β and protein kinase A at Thr212 and Ser214 generates the Alzheimer-specific epitope of antibody AT100 and requires a paired-helical-filament-like conformation. Eur. J. Biochem. **252:**542–552.

64. **Zhou, F. Q., J. Zhou, S. Dedhar, Y. H. Wu, and W. D. Snider.** 2004. NGF-induced axon growth is mediated by localized inactivation of GSK-3β and functions of the microtubule plus end binding protein APC. Neuron **42:**897–912.